IEEE Journal of Microwaves

Received 19 October 2023; revised 27 November 2023; accepted 18 December 2023. Date of publication 5 January 2024; date of current version 9 April 2024.

Digital Object Identifier 10.1109/JMW.2023.3345133

Murine Skin Dosimetry Under Millimeter Wave Exposure

SERAFEIM IAKOVIDIS [1,2], SIMONA LEONARDI [3], EMILIANO FRATINI [3], SIMONETTA PAZZAGLIA [3], MARIATERESA MANCUSO [3], AND THEODOROS SAMARAS [1,2] (Member, IEEE)

(Regular Paper)

[1]CIRI – Center for Interdisciplinary Research and Innovation, Aristotle University of Thessaloniki, 57001 Thessaloniki, Greece
[2]Radiocommunications Lab, Department of Physics, Aristotle University of Thessaloniki, 54124 Thessaloniki, Greece
[3]Division of Health Protection Technologies, Agenzia Nazionale per le Nuove Tecnologie, l'Energia e lo Sviluppo Economico Sostenibile (ENEA), 00196 Roma, Italy

CORRESPONDING AUTHOR: Serafeim Iakovidis (e-mail: siako@physics.auth.gr).

This work was supported by the European Union's Horizon Europe Framework Programme under Grant Agreement number 101057622 (Project SEAWave).

This work involved human subjects or animals in its research. Approval of all ethical and experimental procedures and protocols was granted by the local Ethical Committee for Animal Experiments of the ENEA under Application No. 107/2023-PR, and performed in line with the European Community Council Directive 2010/63/EU.

ABSTRACT The upper part of the frequency spectrum (millimeter waves, MMW) applied by modern communications technologies (5G and beyond), makes skin the dominantly exposed tissue to electromagnetic fields. In this work, a methodology for murine skin dosimetry evaluation is presented, intended to contribute to animal studies with mice exposed to MMW radiation, in particular 27.5 GHz. A stratified skin model is proposed and the variations of the skin layers' thicknesses during a hair cycle are measured in mice. The variations of skin layers' dielectric properties due to age, based on the changes of total body water, are also evaluated. The impact of these variations in dosimetric metrics (i.e., mean absorbed power density, APD, and power loss) within each layer is assessed and found to be significant. Changes in the skin layers' thicknesses throughout a hair cycle considerably affect the APD, resulting in a two-fold increase, compared to changes in the dielectric properties due to aging or due to hair presence inside the skin.

INDEX TERMS Dosimetry, electromagnetic fields, EMF, 5G, murine skin, mice, millimeter waves, MMW.

I. INTRODUCTION

The evolution of mobile communications facing new demands regarding speed (high-data rates), synchronization (low-latency), and the number of connected devices (IoT), has led the industry to use the upper part of the frequency spectrum (millimeter waves, MMW). Compared to the well-studied lower part of the frequency spectrum, MMW electromagnetic fields impose new challenges to the study of potential health effects on humans. Their shorter wavelength results in significantly lower penetration depth in human tissues [1]. Thus, skin, as the outermost tissue of the human body, is dominantly exposed and consequently studied [2]. Skin is an organ with a highly complex anatomy involving different types of cells at different depths. Moreover, it is an organ with a dynamic anatomy, since the distribution of these different types of cells changes with time (e.g., keratinization, hair cycle).

A large number of dosimetry studies on human skin is available in the literature, [1], [3], [4], [5], [6], [7], [8], [9], [10], [11], [12]. A stratified model of human skin is applied in most of them [1], [3], [4], [5], [6], [8], [9], [10], [11], [12], distinguishing between different skin layers (i.e., Stratum Corneum, Epidermis, Dermis) and underlying tissues (i.e., Subcutaneous Fat, Muscle). Some of them also investigate the impact of skin appendages on dosimetry, like sweat glands [6], [7], [8], [12] or others [5]. The impact of variations of skin strata thicknesses [1], [3], [4], [9], [10], [11], or dielectric properties with age [9] in dosimetry, has also been studied.

A significant number of studies dealing with dosimetry of rodents (i.e., rats and mice) is already available in the liter-

ature, [13], [14], [15], [16], [17], [18], [19], [20], [21], [22], but most of them focus on specific exposure setups used for animal studies [13], [14], [16], [17], [18], [19], [21], [22] for frequencies lower than that of MMW. Consequently, exposure specific to murine skin has not been investigated. In [20], MMW frequencies (i.e., 37-74 GHz) are considered and a stratified skin model is applied for dosimetry evaluation. In [15], variation of dielectric properties in rats' tissues with age is evaluated. In this work, for the first time, a method for the dosimetric evaluation of murine skin exposure to MMW (27.5 GHz) is presented, considering the variations of skin strata thicknesses and dielectric properties with age and hair presence inside the skin. The aim of the current work is to contribute to the dosimetry of the animal study, which will be performed within the SEAWave Project [23] focusing on the effects of MMW on the skin. Animal studies investigating the impact of radiofrequency and microwave radiation should report organ-specific dosimetry, especially for the organs and tissues implicated in the biological effects investigated. Therefore, it is necessary to be able to correlate the absorbed power at various depths and locations of cell types with the observed biological endpoints, since different cell types in the skin result in different types of cancer. In MMW frequencies, dosimetry of the skin exposed to radiation is influenced mainly by its structure along wave propagation. In order to study the variability in dosimetry resulting from the variation of skin anatomy it is preferable to use 1-D models, since the size of anatomical structures in the skin and their development in time make 3-D modeling with full-wave simulations prohibitive in terms of computational resources.

II. MATERIALS AND METHODS

The study is focused on mouse skin, since this is the tissue that dominantly absorbs electromagnetic energy at this frequency. To this aim, a planar stratified model of mice skin layers has been considered. An analytical solution of Maxwell's equations for this model is used to evaluate the field values and other relevant dosimetric quantities inside the skin. The implemented analytical solution is validated against both theoretical and experimental data presented in [20]. Exposure variations emanating from changes in skin layers thicknesses and dielectric properties (permittivity, conductivity), due to age and hair content, are also evaluated.

A. MOUSE SKIN MODEL

1) GEOMETRY OF THE MODEL

The mouse skin model developed in this study follows the approach of human skin models already used in dosimetric studies, e.g., [1], [3], [9], [10]. In this context, a planar geometrical structure is used to model mouse skin and underlying tissues, consisting of five different layers (Fig. 1): a) Keratinized stratum (KS), consisting of stratum corneum and stratum lucidum, b) Viable epidermis (VE), c) Dermis (DE), d) Hypodermis (consisting of fat, FT) and e) Muscle (MS).

These layers can be identified in a hematoxylin & eosin (H&E) stained, cross-sectional mouse skin sample image (Fig. 2).

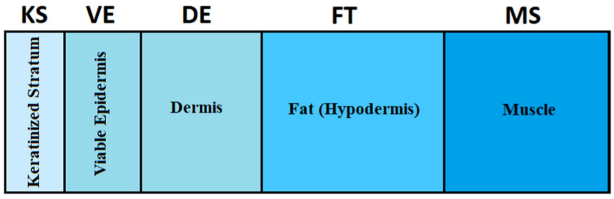

FIGURE 1. Layered model of mouse skin used for dosimetric study.

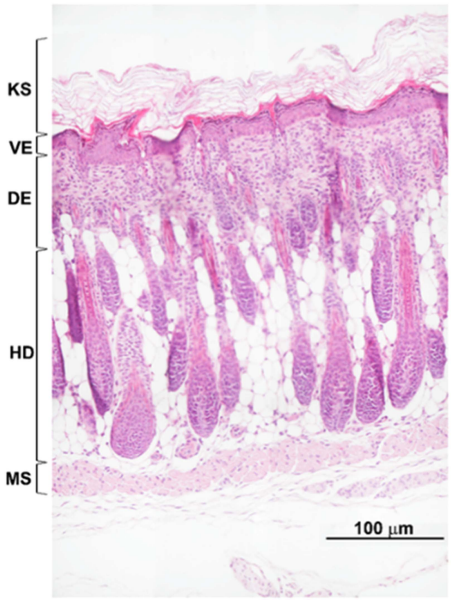

FIGURE 2. Representative image of a cross-sectional mouse skin section at postnatal day 2 and layer identification. KS, keratinized stratum; VE, viable epidermis; DE, dermis; HD, hypodermis; MS, muscle. Scale bar = 100 μm.

For the determination of the skin layers' thicknesses, mean values are available in the literature [24]. However, marked age- and genetic background-dependent variations in mouse skin thickness associated to the hair cycle phase have been observed [25], [26], [27]. The hair cycle is a periodic phenomenon, consisting in phases of growth (anagen), regression (catagen) and rest (telogen), and occurs many times throughout the life period of a mouse. The first hair cycle in particular, largely synchronous, is a crucial period because the hair follicles are actively producing new hairs and establishing the initial pattern and direction of hair growth.

Thus, we focused on the examination of skin during the first hair cycle of CD1 mice, to capture the variations of skin layers' thicknesses. To this aim, dorsal skin samples were collected from mice at different ages, specifically 2, 5, 10, 15 and 21 days old, (n=3 for each age) and processed for histology according to standard procedures. After H&E staining, transversal skin sections were analyzed under a light microscopy and images acquired using the software NIS-Elements BR 4.00.05 (Nikon Instruments Europe B.V.; Florence, Italy).

Fig. 3 reveals that hair follicles begin elongating around the midpoint of the anagen phase (P5), with their length peaking during the late anagen phase (P10). Subsequently, this length

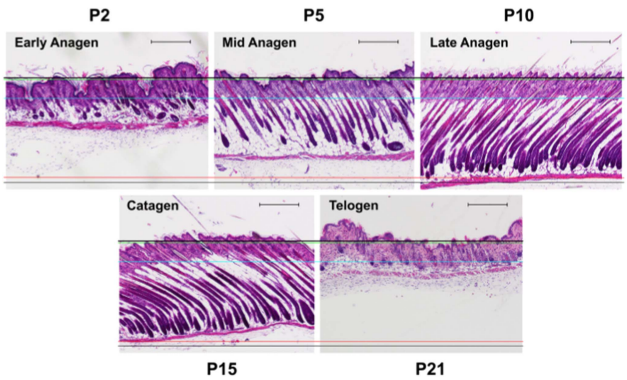

FIGURE 3. H&E-stained images of cross-sectional mouse skin samples at postnatal days 2, 5, 10, 15 and 21 to illustrate the hair cycle phase-dependent variation of thickness during the first hair cycle. Scale bar = 300 μm.

TABLE 1 Measurements of Mouse Skin Layers' Thicknesses During the First Hair Cycle

Postnatal Day	Layer thickness (μm)	Keratinized Stratum	Viable Epidermis	Dermis	Hypodermis	Muscle	Total
P2	mean	69.39	21.57	94.62	134.16	49.11	368.84
	std	5.57	5.10	41.94	49.28	12.46	
P5	mean	45.83	37.91	132.43	514.88	38.51	769.55
	std	6.79	8.86	26.16	81.35	19.12	
P10	mean	50.37	23.16	169.34	644.14	42.39	929.40
	std	6.57	4.68	12.42	68.64	8.21	
P15	mean	16.14	18.46	149.49	597.14	19.21	800.93
	std	2.84	4.69	20.42	45.08	2.49	
P21	mean	14.45	16.33	183.14	63.59	50.05	327.57
	std	3.35	3.94	43.63	31.30	24.73	

gradually diminishes until it reaches its minimum during the telogen phase (P21).

For each mouse skin sample, 12 measurements were taken for each skin compartment, according to Fig. 2. The results of the measurements for the different skin layers as a function of the mouse age are summarized in Table 1.

2) DIELECTRIC PROPERTIES OF TISSUE LAYERS

The dielectric properties of murine skin found in [20] were used. In [20], skin samples of both shaved hairy and hairless mice were studied. The measured power reflection coefficient was higher in hairless compared to hairy, even shaved, mice. This was attributed to the volume that the hairs occupy within the hairy skin, thus decreasing the effective free water content of skin, since hairs do not contain free water. As a result, in [20], the estimated dielectric properties for epidermis and dermis layers were found different for hairy and hairless mice. The results in [20], clearly suggest that the hair volume content of the viable epidermis and dermis affects the dielectric properties of these two layers. In addition, measurements of the hair volume content in different postnatal days (P2-P21) show a variation during a hair cycle in the range of 1.06%-3.16% V/V, for viable epidermis and dermis layers. In order to estimate the corresponding dielectric properties' variation, we applied Lichtenecker's mixing formula:

$$\varepsilon_L^k = f_1 \cdot \varepsilon_1^k + f_2 \cdot \varepsilon_2^k \tag{1}$$

where ε_L is the permittivity of the dielectric mixture, ε_1 is the permittivity of the first component (i.e., viable epidermis-dermis of hairless mice), ε_2 is the permittivity of the second component (i.e., hair) and f_1, f_2 are the volume contents of the first and second components of the composite/mixture ($f_1 + f_2 = 1$), respectively. Each value of k describes a specific microgeometry (topology) of a composite [28]. Parameter k varies within the $[-1,1]$ range, describing a transition from anisotropy for $k = -1$ to anisotropy for $k = 1$. The two extreme values of k (i.e., -1 and 1) correspond to two 'extreme' topologies of the composite material, regarding its interaction with electromagnetic fields: Both components are considered parallel plates either parallel (k= -1) or perpendicular (k = 1) to the incident electric field [29].

In order to test the applicability of the Lichtenecker mixing formula to our case, we applied the formula to our mixture (i.e., viable epidermis-dermis of hairless mice and hair) using the values of dielectric properties from [20] and compared the results with the ones given for hairy mouse, also in [20]. Note that, following the approach in [20], we consider the same dielectric properties for both viable epidermis and dermis layers. The complex permittivity considered for hair was [5], [30]:

$$\varepsilon_{hair} = 2.6 - 0.1j \tag{2}$$

Our calculations show that the application of Lichtenecker's formula to a composite made of hairs embedded in hairless mice skin can adequately predict the dielectric properties of hairy mice (deviation $< 0.5\%$) for all three different frequencies examined (i.e., 40 GHz, 50 GHz and 60 GHz). It is remarkable that the best fit of the data for all three frequencies was achieved for the same values of k and f_2, namely $k = 0.11$ and $f_2 = 0.03$ or 3% V/V of hairs in the skin. This is an expected result, since neither the topology (k) nor the hair volume content (f_2) of the skin samples measured in [20] changes with frequency.

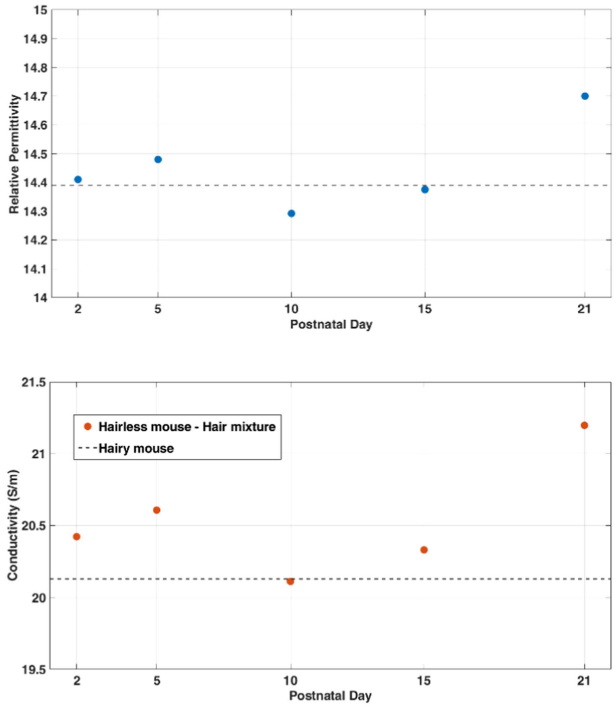

FIGURE 4. Relative permittivity (top, blue points) and conductivity (bottom, red points) during a hair cycle (viable epidermis and dermis) for a mixture of hairless mouse skin layers with hairs. Conductivity and relative permittivity values for hairy mouse in [20] are also plotted (black dashed lines).

Using the value of k ($k = 0.11$) estimated above and the hair volume content of epidermis and dermis layers measured in mice skin samples at different postnatal days (P2-P21), we evaluated the variability of the dielectric properties for these layers during a hair cycle, Fig. 4.

It's worth mentioning that this variability emanates from the hair volume content variability alone. As will be shown later, this variability is not significant compared to the one emanating from the Total Body Water (TBW) variation with age (i.e., postnatal day). Consequently, it is not taken into account in dosimetry evaluations hereafter.

The Swiss Webster (hairy) mouse values were applied in the current study. The one-term Debye model [20] was used to calculate the properties for the frequency considered in this work (27.5 GHz). The dielectric properties for fat and muscle layer of [1], [31] were also used. The applied values are summarized in Table 2.

It should be mentioned here that the dielectric properties values reported in Table 2 correspond to individuals of a specific age. However, it is known that these properties vary with age [9], [15], [32]. In the gigahertz frequency range, electromagnetic fields interaction with tissues dominantly results from free water molecule polarization (γ-dispersion) [3]. The water content of tissues varies with age and so do their dielectric properties. In this context, the Total Body Water (TBW), defined as the ratio of the mass of the water in an individual's body to the total mass of the body, is used as a

TABLE 2 Dielectric Properties Assumed for Mouse Skin at 27.5 GHz

Skin Layer	Relative Permittivity	Conductivity (S/m)
KS (Keratinized Stratum)	3.39	0
VE (Viable Epidermis)	14.39	20.13
DE (Dermis)	14.39	20.13
FT (Fat)	3.54	2.19
MS (Muscle)	23.53	37.42

proxy for the evaluation of variations of the dielectric properties with age [9], [32]. Wang et al. [32] applied Lichtenecker's logarithmic Formula (3), considering tissues as a mixture of organic material and water.

$$\varepsilon_r = \varepsilon_{rw}^{\alpha} \cdot \varepsilon_{rt}^{1-\alpha} \tag{3}$$

where ε_{rw} is the relative permittivity of water, ε_{rt} is the relative permittivity of the organic material and α is the hydrated rate ($\alpha = \rho \cdot \text{TBW}$, where ρ is the mass density). Since the relative complex permittivity of a tissue $\dot{\varepsilon}_r$ is given by

$$\dot{\varepsilon}_r = \varepsilon'_r - j\varepsilon''_r = \varepsilon_r - j\frac{\sigma}{\omega\varepsilon_0} = \varepsilon_r\left(1 - j\frac{1}{\omega\tau}\right) \tag{4}$$

substituting (4) into (3) results in

$$\dot{\varepsilon}_r = \varepsilon_{rw}^{\frac{\alpha-\alpha_A}{1-\alpha_A}} \cdot \varepsilon_{rA}^{\frac{1-\alpha}{1-\alpha_A}}\left(1 - j\frac{1}{\omega\tau}\right) \tag{5}$$

where ε_{rA} is the relative permittivity for tissue at age A and α_A is the hydrated rate for tissue at age A. Equation (5) gives the complex permittivity at different ages, if the TBW as a function of age is known and the dielectric properties at age A are also known. This approach was followed by Sacco et al. [9] to evaluate the age-dependence of electromagnetic power deposition in human skin. The authors considered no variations of TBW on the outermost skin layer (i.e., SC) with age, since this layer is mostly impacted by environmental and physiological conditions.

Following the approach of Wang [32] and Sacco [9], and considering that the dielectric properties of the skin layers at age A are known (Table 2), it was necessary to determine the TBW of mice as a function of age in the literature. In [33], Bailey et al. studied the body composition of 111 white male mice in terms of protein, water, fat and ash as a function of age. Data for only 16 of them are published. Curve fitting of these data, using the least square method, resulted in the equation:

$$\text{TBW} = -2.93 \cdot \ln(\text{age}) + 79.97 \tag{6}$$

where TBW is evaluated in terms of percentage and age in terms of postnatal days. The relative permittivity of water was

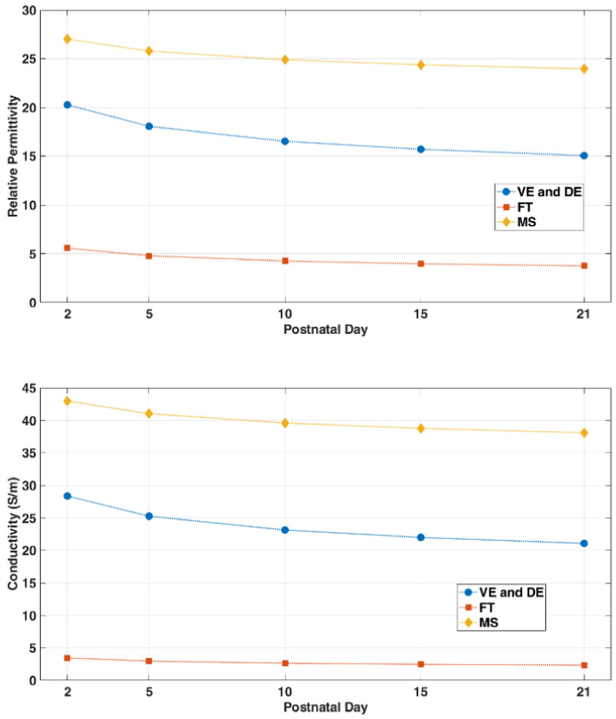

FIGURE 5. Relative permittivity (top) and conductivity (bottom) vs postnatal age for mouse skin layers (viable epidermis, dermis, fat and muscle) due to changes in TBW.

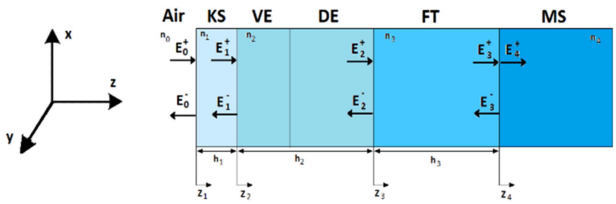

FIGURE 6. Stratified mouse skin model used for electromagnetic analysis.

evaluated using the Ellison et al. model [34], for a temperature of 32.8 °C [20], while the mass density values in [9] for each skin layer were used. To determine the age A of the mice at which the dielectric properties were assessed, we made the approximation of A = 28 days, based on the reported weight range in [20] (i.e., 20-25 g) and the growth chart provided [35]. The variation of dielectric properties as a function of age (postnatal days) for the considered skin layers is plotted in Fig. 5.

This variation originates from the change of TBW with age and it is significant during the first days of life. The dielectric properties tend to a constant value after several postnatal days.

B. COMPUTATIONAL METHOD

The stratified mouse skin model presented in Fig. 1 was used for the electromagnetic analysis. The model considered here is irradiated with a TEM-polarized plane wave (Fig. 6).

The direction of the propagation (along z-axis) is perpendicular to the interfaces of the skin layers. The electric (E) and magnetic (H) field values are calculated analytically using

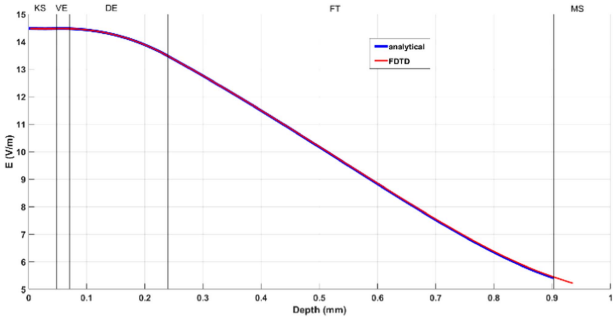

FIGURE 7. Model verification: E field values comparison, using the analytical and the FDTD method. Frequency 27.5 GHz, incident power density 1 W/m^2, normal incidence of TEM wave, median layers' thicknesses for postnatal day 10.

the transmission and reflection coefficients at all tissue interfaces [36]. The muscle layer is considered as the terminating layer, i.e., no reflections at the tissue interfaces underlying the muscle layer are taken into account. This approach has already been applied successfully in previous studies [4], [9], [10] and offers an important speed advantage over other computational methods (e.g., FDTD, FEM). The calculations were performed with MATLAB (The MathWorks Inc., Natick, MA, USA).

C. METHOD VALIDATION

The developed method and corresponding MATLAB code was initially verified against a commercially available software (Sim4Life, ZMT, Switzerland) which implements the FDTD method (Fig. 7).

A stratified model of skin was also used with the FDTD method. Periodic boundary conditions were used on the sides and perfectly matched layers on top and bottom. The model was irradiated with a TEM plane wave of incident power density of 1 W/m^2 in air. As can be inferred from Fig. 7, the results using the two methods are in a very good agreement (deviation $< 2\%$).

We tested our method against the results (both theoretical and experimental) presented in [20]. Alekseev et al. measured the power reflection coefficients of both shaved hairy and hairless mouse skin samples using waveguides, in the 37-74 GHz frequency range. Additionally, they evaluated all the parameter values (skin layers dimensions, dielectric properties) that give the best fit of their model to the experimental data. The results for the hairy murine skin only are presented in chart form (Fig. 1 in [20]). Lacking the exact data, we digitized this chart and tried to reproduce the results using our model by applying the same parameter values (skin layers dimensions, dielectric properties) as in [20], (Fig. 8).

The results obtained with our method appear to be in good agreement with both theoretical and experimental data in [20]. It should be noted here that the two different branches of the curve in Fig. 8 (37–53 GHz and 54–74 GHz) stem from the fact that two different rectangular waveguides were used for the measurements performed by Alekseev et al. The first

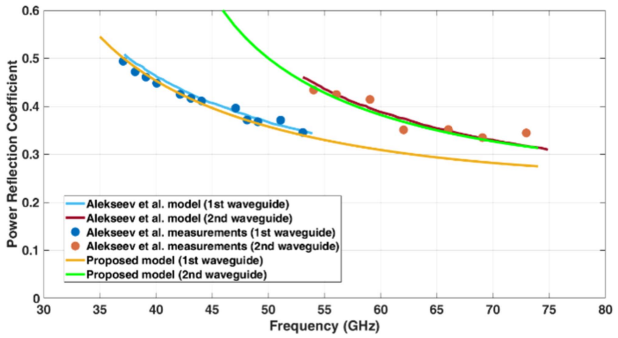

FIGURE 8. Comparison of the power reflection coefficient as evaluated from the proposed model in this work (yellow, green lines) and from the model (blue, brown lines) and measurements (blue, brown circles) in [20].

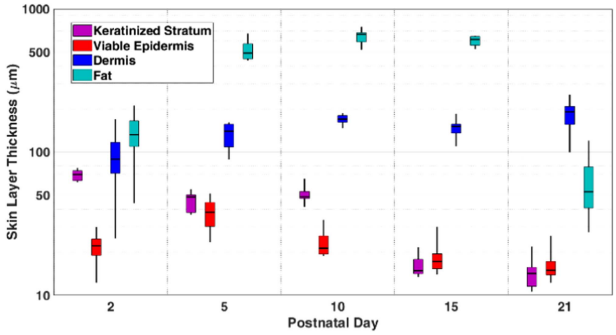

FIGURE 9. Skin layers' thickness at different postnatal days (2-21): Median (red line), interquartile range (blue box) and min-max values (dotted black line). KS: Keratinized stratum, VE: Viable epidermis, DE: Dermis, FT: Fat.

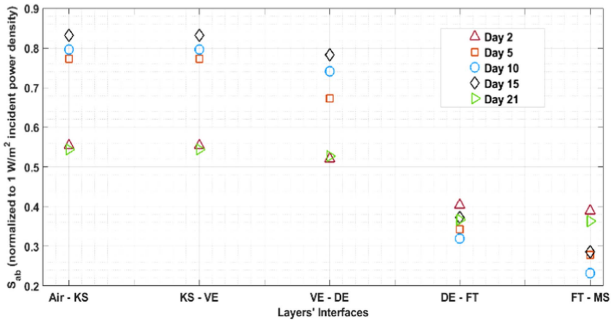

FIGURE 10. APD, S_{ab}, at skin layer interfaces for different postnatal days.

waveguide (37–53 GHz) had dimensions of 5.2 mm × 2.6 mm with a cutoff wavelength of $\lambda_{c1} = 10.4$ mm, while the second one (54–74 GHz) had dimensions of 3.6 mm × 1.8 mm with $\lambda_{c1} = 7.2$ mm, [3]. The application of the effective permittivity (as suggested in [3]) which is a function of cutoff wavelength, leads to the two different branches of Fig. 8, one for each of the two different waveguides used in [20].

D. DOSIMETRIC QUANTITIES

According to the International Commission on Non-Ionizing Radiation Protection (ICNIRP), the absorbed power density (APD) level, S_{ab} (W/m^2), is considered the relevant metric for the basic restriction for frequencies higher than 6 GHz [37]. Consequently, S_{ab} is evaluated at the interfaces of the skin layers by using the formula based on the Poynting vector:

$$S_{ab} = \iint_A Re\,[\boldsymbol{S}] \cdot \frac{d\boldsymbol{s}}{A} = \iint_A Re\left[\boldsymbol{E} \times \boldsymbol{H}^*\right] \cdot \frac{d\boldsymbol{s}}{A} \tag{7}$$

The mean value of absorbed power density within each skin layer, $\overline{S_{ab}}$, is also evaluated:

$$\overline{S_{ab}} = \frac{\int_{z_1}^{z_2} S_{ab}(z)\,dz}{\int_{z_1}^{z_2} dz} \tag{8}$$

where z_1, z_2 are the coordinates of the boundaries of the considered layer. The power loss per normal surface area within each layer of the skin is, then, calculated by the difference of the APD entering the layer minus the APD leaving it:

$$\mathrm{PL} = S_{ab}(z_2) - S_{ab}(z_1) \tag{9}$$

III. RESULTS AND DISCUSSION

The dosimetric study of mouse skin is focused on the first hair cycle (postnatal days 2–21). The reason for the selection of this time period of mouse life is twofold: a) The largest variability of layers' thicknesses occurs during this period (Fig. 3). b) The largest variability of the dielectric properties of mouse skin layers due to water content also occurs during this period (Fig. 5). Consequently, the APD and the PL are expected to vary more during this time period compared to any other. Therefore, the study of this time period provides the safest way to evaluate the worst-case scenario for the temporal variations of absorbed power.

The variability of the skin layers' thicknesses during the first hair cycle is presented in Fig. 9. Thickness values correspond to four different skin samples for each of the three different individual animals measured at five different postnatal days. Thus, the variability presented in Fig. 9 originates from sampling uncertainty (four different evaluation points) and interindividual variability (three different mice), which also includes sex variability, since the three mice are of both sexes (not only male or only female). The significant variation of the skin layers' thicknesses throughout a hair cycle, dominated by the variation of the subcutaneous fat layer, presented in the literature (Fig. 3), is confirmed by the measurement results shown in Fig. 9.

First, the absorbed power density (APD) at layers' interfaces is evaluated (Fig. 10) by using the median values for the layers' thicknesses at different postnatal days (Fig. 9) and by setting the layers' dielectric properties to the values found in the literature for animals at age A (i.e., 28 days). Large variations of the APD (S_{ab}) are observed during the first hair cycle. These can be attributed to the large variations of skin layers' thicknesses.

In Fig. 11 the distribution of power loss in each of the skin layers (KS, VE, DE and FT) due to the variability of the layers' thicknesses (Fig. 9) is presented using boxplot charts when the dielectric constants are kept constant with postnatal age (i.e., at 28 days, as found in the literature). The same distribution (of power loss) is depicted in Fig. 11 when the dielectric properties of the layers change with age (due to the change in TBW) in addition to the layers' thicknesses. The

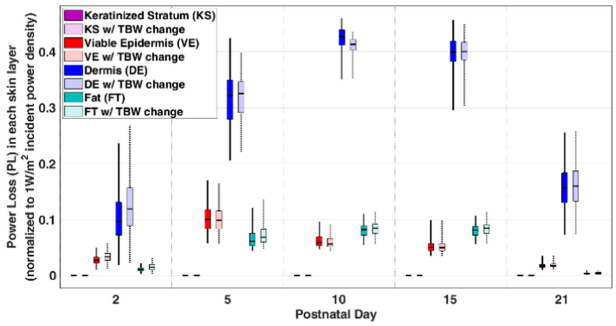

FIGURE 11. Power loss, PL, within each skin layer (KS, VE, DE, FT), on different postnatal days for constant dielectric properties (dark-colored boxes) and for dielectric properties changing with age, i.e., with TBW (light-colored boxes with dotted whiskers).

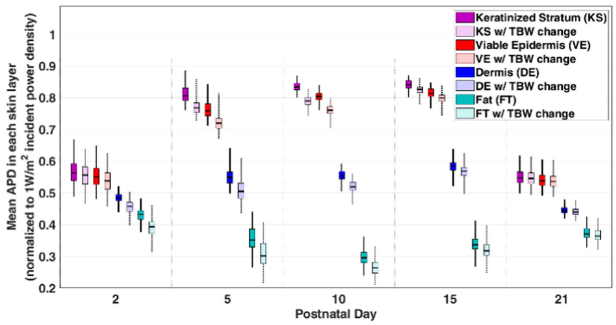

FIGURE 12. Mean APD, $\overline{S_{ab}}$, within each skin layer (KS, VE, DE, FT), on different postnatal days for constant dielectric properties (dark-colored boxes) and for dielectric properties changing with age, i.e., with TBW (light-colored boxes with dotted whiskers).

comparison shows that the impact of considering dielectric variations with age has a much lower impact on the power loss within each skin layer compared to the impact that the variation of the skin layers' thicknesses has during the first hair cycle. The maximum power per normal surface area deposited within any skin layer and for any postnatal day is 0.45 W/m^2 (dermis layer on postnatal day 15) for incident power density of 1 W/m^2.

In Fig. 12 the distribution of the mean APD, $\overline{S_{ab}}$ (8), within each skin layer is presented. The mean APD is progressively decreasing as depth increases, as expected (Fig. 10). Again, the impact of considering dielectric properties variations with age is much lower compared to that originating from the skin layers' thicknesses variation.

Organ-specific dosimetry is an important aspect of biological experiments with animals addressing the health risk concerns of wireless communications. Kuster and Schönborn [38] in their guidelines recommend that the experimental setup should enable an accurate description of the distribution and magnitude of the induced fields inside the different tissues and organs. This is particularly important in cases where the biological responses of specific organs/tissues are being investigated [39]. Therefore, for frequencies that can penetrate deep in the body of the animals, the organ-averaged specific absorption rate (oSAR) provides an acceptable proxy of exposure quantification for risk assessment purposes [21], [39], [40]. In MMW the absorption of energy is of concern mainly for the skin, i.e., a single organ. However, this organ presents a structure which entails various types of cells that result in different biological responses. Therefore, it should be attempted to characterize exposure of each cell type, if possible. To achieve this, the stratified structure of the skin can be exploited. Reported oSAR can have considerable variability due to uncertainty of the geometrical/anatomical representation of the animal and uncertainty of the dielectric parameters assigned to the different tissues/organs [39]. Similarly, the dosimetry at the skin layers' scale can vary considerably due to the anatomical and physiological changes that affect the values of the layers' thicknesses and dielectric properties, as described above.

IV. CONCLUSION

A dosimetric study for mouse skin irradiated at 27.5 GHz and normal incidence was performed. The study was performed at the macroscopic scale, taking into account (for the first time) the variation of skin layers' thicknesses due to the hair cycle and the changes in the dielectric properties due to age (and, correspondingly, water content) and the hair cycle. It was shown that the impact of layer thickness variation on dosimetric metrics is significantly larger compared to the one of dielectric properties. The full dosimetric evaluation of animals during a long-term study needs to consider also the layer of fur at different time periods (hair cycle) and conditions (wet and dry), on which work is ongoing.

COMPLIANCE WITH REGULATIONS

This animal study was performed according to the European Community Council Directive 2010/63/EU, approved by the local Ethical Committee for Animal Experiments of the ENEA, and authorized by the Italian Ministry of Health (n° 107/2023-PR).

REFERENCES

[1] M. C. Ziskin, S. I. Alekseev, K. R. Foster, and Q. Balzano, "Tissue models for RF exposure evaluation at frequencies above 6 GHz," *Bioelectromagnetics*, vol. 39, no. 3, pp. 173–189, Apr. 2018, doi: 10.1002/bem.22110.

[2] T. Wu, T. S. Rappaport, and C. M. Collins, "Safe for generations to come: Considerations of safety for millimeter waves in wireless communications," *IEEE Microw. Mag.*, vol. 16, no. 2, pp. 65–84, Mar. 2015, doi: 10.1109/MMM.2014.2377587.

[3] S. I. Alekseev and M. C. Ziskin, "Human skin permittivity determined by millimeter wave reflection measurements," *Bioelectromagnetics*, vol. 28, no. 5, pp. 331–339, Jul. 2007, doi: 10.1002/bem.20308.

[4] A. Christ, T. Samaras, E. Neufeld, and N. Kuster, "Transmission coefficient of power density into skin tissue between 6 and 300 GHz," *Radiat. Protection Dosimetry*, vol. 192, no. 1, pp. 113–118, Oct. 2020, doi: 10.1093/rpd/ncaa179.

[5] Z. Haider, Y. Le Drean, G. Sacco, D. Nikolayev, R. Sauleau, and M. Zhadobov, "High-resolution model of human skin appendages for electromagnetic dosimetry at millimeter waves," *IEEE J. Microwaves*, vol. 2, no. 1, pp. 214–227, Jan. 2022, doi: 10.1109/jmw.2021.3126712.

[6] Z. Vilagosh, N. Foroughimehr, A. Lajevardipour, and A. W. Wood, "FDTD simulations of sweat ducts and hair at 0.45 THz," *Dermato*, vol. 3, no. 1, pp. 69–84, Mar. 2023, doi: 10.3390/dermato3010006.

[7] A. R. Eldamak, S. Thorson, and E. C. Fear, "Study of the dielectric properties of artificial sweat mixtures at microwave frequencies," *Biosensors*, vol. 10, no. 6, Jun. 2020, Art. no. 62, doi: 10.3390/BIOS10060062.

[8] Y. Feldman, A. Puzenko, P. B. Ishai, A. Caduff, and A. J. Agranat, "Human skin as arrays of helical antennas in the millimeter and submillimeter wave range," in *Proc. 33rd Int. Conf. Infrared, Millimeter THz Waves*, 2008, pp. 1–2, doi: 10.1109/ICIMW.2008.4665663.

[9] G. Sacco, S. Pisa, and M. Zhadobov, "Age-dependence of electromagnetic power and heat deposition in near-surface tissues in emerging 5G bands," *Sci. Rep.*, vol. 11, no. 1, Dec. 2021, Art. no. 3983, doi: 10.1038/s41598-021-82458-z.

[10] A. Christ, T. Samaras, E. Neufeld, and N. Kuster, "RF-induced temperature increase in a stratified model of the skin for plane-wave exposure at 6–100 GHz," *Radiat. Protection Dosimetry*, vol. 188, no. 3, pp. 350–360, Jun. 2020, doi: 10.1093/rpd/ncz293.

[11] A. Christ, A. Aeschbacher, F. Rouholahnejad, T. Samaras, B. Tarigan, and N. Kuster, "Reflection properties of the human skin from 40 to 110 GHz: A confirmation study," *Bioelectromagnetics*, vol. 42, no. 7, pp. 562–574, Oct. 2021, doi: 10.1002/bem.22362.

[12] G. Shafirstein and E. G. Moros, "Modelling millimetre wave propagation and absorption in a high resolution skin model: The effect of sweat glands," *Phys. Med. Biol.*, vol. 56, no. 5, pp. 1329–1339, Mar. 2011, doi: 10.1088/0031-9155/56/5/007.

[13] F. Schönborn, K. Poković, and N. Kuster, "Dosimetric analysis of the carousel setup for the exposure of rats at 1.62 GHz," *Bioelectromagnetics*, vol. 25, no. 1, pp. 16–26, Jan. 2004, doi: 10.1002/bem.10153.

[14] L. B. Sasser, J. E. Morris, B. W. Wilson, and L. E. Anderson, "Genotoxic potential of 1.6 GHz wireless communication signal: *In Vivo* two-year bioassay," *Radiat. Res.*, vol. 159, no. 4, pp. 558–564, Apr. 2003, doi: 10.1667/0033-7587(2003)159[0558:GPOGWC]2.0.CO;2.

[15] A. Peyman, A. A. Rezazadeh, and C. Gabriel, "Changes in the dielectric properties of rat tissue as a function of age at microwave frequencies," 2001. [Online]. Available: www.iop.org/Journals/pbPII:S0031-9155

[16] T. Wu, A. Hadjem, M. F. Wong, A. Gati, O. Picon, and J. Wiart, "Whole-body new-born and young rats' exposure assessment in a reverberating chamber operating at 2.4 GHz," *Phys. Med. Biol.*, vol. 55, no. 6, pp. 1619–1630, 2010, doi: 10.1088/0031-9155/55/6/006.

[17] R. Pinto et al., "Dosimetry of a set-up for the exposure of newborn mice to 2.45-GHz WIFI frequencies," *Radiat. Protection Dosimetry*, vol. 140, no. 4, pp. 326–332, Apr. 2010, doi: 10.1093/rpd/ncq129.

[18] L. Ardoino, V. Lopresto, S. Mancini, C. Marino, R. Pinto, and G. A. Lovisolo, "A radio-frequency system for in vivo pilot experiments aimed at the studies on biological effects of electromagnetic fields," *Phys. Med. Biol.*, vol. 50, no. 15, pp. 3643–3654, Aug. 2005, doi: 10.1088/0031-9155/50/15/011.

[19] A. K. Fall, C. Lemoine, P. Besnier, R. Sauleau, Y. L. Dréan, and M. Zhadobov, "Exposure assessment in millimeter-wave reverberation chamber using murine phantoms," *Bioelectromagnetics*, vol. 41, no. 2, pp. 121–135, Feb. 2020, doi: 10.1002/bem.22243.

[20] S. I. Alekseev, O. V. Gordiienko, and M. C. Ziskin, "Reflection and penetration depth of millimeter waves in murine skin," *Bioelectromagnetics*, vol. 29, no. 5, pp. 340–344, Jul. 2008, doi: 10.1002/bem.20401.

[21] Y. Gong et al., "Life-time dosimetric assessment for mice and rats exposed in reverberation chambers for the two-year NTP cancer bioassay study on cell phone radiation," *IEEE Trans. Electromagn. Compat.*, vol. 59, no. 6, pp. 1798–1808, Dec. 2017, doi: 10.1109/TEMC.2017.2665039.

[22] V. De Santis, A. Di Fracesco, K. R. Foster, G. Bit-Babik, and A. Faraone, "Monte-Carlo based numerical dosimetry in reverberation chamber exposure systems employed for in-vivo rodent bioassays," *IEEE Access*, vol. 11, pp. 22018–22033, 2023, doi: 10.1109/ACCESS.2023.3251889.

[23] "SEAWave project," 2023. Accessed: Sep. 28, 2023. [Online]. Available: https://seawave-project.eu/

[24] N. A. Monteiro-Riviere, D. G. Bristol, T. O. Manning, R. A. Rogers, and J. E. Riviere, "Interspecies and interregional analysis of the comparative histologic thickness and laser Doppler blood flow measurements at five cutaneous sites in nine species," *J. Invest. Dermatol.*, vol. 95, no. 5, pp. 582–586, 1990, doi: 10.1111/1523-1747.ep12505567.

[25] H. B. Chase, W. Montagna, and J. D. Malone, "Changes in the skin in relation to the hair growth cycle," *Anat. Rec.*, vol. 116, no. 1, pp. 75–81, 1953, doi: 10.1002/ar.1091160107.

[26] L. S. Hansen, J. E. Coggle, J. Wells, and M. W. Charles, "The influence of the hair cycle on the thickness of mouse skin," *Anat. Rec.*, vol. 210, no. 4, pp. 569–573, 1984, doi: 10.1002/ar.1092100404.

[27] S. Müller-Röver et al., "A comprehensive guide for the accurate classification of murine hair follicles in distinct hair cycle stages," *J. Invest. Dermatol.*, vol. 117, no. 1, pp. 3–15, 2001, doi: 10.1046/j.0022-202x.2001.01377.x.

[28] A. V. Goncharenko, V. Z. Lozovski, and E. F. Venger, "Lichtenecker's equation: Applicability and limitations," 2000. [Online]. Available: www.elsevier.comrlocateroptcom

[29] D. J. Bergman, "The dielectric constant of a composite material—A problem in classical physics," *Phys. Rep.*, vol. 43, pp. 377–407, 1978.

[30] S. I. Alekseev and M. C. Ziskin, "Distortion of millimeter-wave absorption in biological media due to presence of thermocouples and other objects," *IEEE Trans. Biomed. Eng.*, vol. 48, no. 9, pp. 1013–1019, Sep. 2001.

[31] P. Weddle et al., "The dielectric properties of biological tissues: II. Measurements in the frequency range 10 Hz to 20 GHz," 1996.

[32] J. Wang, O. Fujiwara, and S. Watanabe, "Approximation of aging effect on dielectric tissue properties for SAR assessment of mobile telephones," *IEEE Trans. Electromagn. Compat.*, vol. 48, no. 2, pp. 408–413, May 2006, doi: 10.1109/TEMC.2006.874085.

[33] C. B. Bailey, W. D. Kitts, and A. J. Wood, "Changes in the gross chemical composition of the mouse during growth in relation to the assessment of physiological age," *Can. J. Animal Sci.*, vol. 40, no. 2, pp. 143–155, 1960, doi: 10.4141/cjas60-022.

[34] W. J. Ellison, "Permittivity of pure water, at standard atmospheric pressure, over the frequency range 0-25 THz and the temperature range –100 °C," *J. Phys. Chem. Reference Data*, vol. 36, no. 1, pp. 1–18, 2007, doi: 10.1063/1.2360986.

[35] "TACONIC, swiss webster growth chart," 2023. Accessed: May 24, 2023. [Online]. Available: https://www.taconic.com/mouse-model/swiss-webster

[36] S. J. Orfanidis and T. Monica, "Electromagnetic waves and antennas," 1999. [Online]. Available: www.ece.rutgers.edu/∼orfanidi/ewa

[37] G. Ziegelberger et al., "Guidelines for limiting exposure to electromagnetic fields (100 kHz to 300 GHz)," *Health Phys.*, vol. 118, no. 5, pp. 483–524, May 2020, doi: 10.1097/HP.0000000000001210.

[38] N. Kuster and F. Schönborn, "Recommended minimal requirements and development guidelines for exposure setups of bioexperiments addressing the health risk concern of wireless communications," *Bioelectromagnetics*, vol. 21, no. 7, pp. 508–514, 2000, doi: 10.1002/1521-186X(200010)21:7<508::AID-BEM4>3.0.CO;2-F.

[39] N. Kuster, V. B. Torres, N. Nikoloski, M. Frauscher, and W. Kainz, "Methodology of detailed dosimetry and treatment of uncertainty and variations for in vivo studies," *Bioelectromagnetics*, vol. 27, no. 5, pp. 378–391, 2006, doi: 10.1002/bem.20219.

[40] Y. Gong, M. Capstick, T. Tillmann, C. Dasenbrock, T. Samaras, and N. Kuster, "Desktop exposure system and dosimetry for small scale in vivo radiofrequency exposure experiments," *Bioelectromagnetics*, vol. 37, no. 1, pp. 49–61, Jan. 2016, doi: 10.1002/bem.21950.

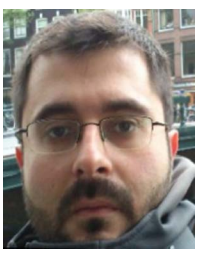

SERAFEIM IAKOVIDIS was born in Thessaloniki, Greece, in 1981. He received the bachelor's degree in physics and the master's degree in electronic physics (radioelectrology) from the Aristotle University of Thessaloniki, Thessaloniki, Greece, in 2004 and 2008, respectively. Since 2009, he has been a member of the Radiocommunications Laboratory, working on electromagnetic field (EMF) exposure assessment. Since 2018, he has also been a member of the EMMETRON team in the Center of Interdisciplinary Research, Aristotle University of Thessaloniki. His research focuses on dosimetry of EMF at MMW frequencies. He is actively involved in the SEAWave Project.

SIMONA LEONARDI born in Palermo, Italy, in 1975. She received the degree in biological sciences from the University "La Sapienza" of Rome, Rome, Italy, in 2004. During her studies, she conducted research on the molecular mechanisms involved in skin tumor development using various mouse models with the Biotechnology Unit of ENEA. Since 2012, she has held the position of Junior Scientist with ENEA, where her primary focus has been the investigation of the health effects of low doses of ionizing radiation using experimental mouse models. She has authored or coauthored 23 scientific publications. Her expertise spans histology and molecular biology, with a specific emphasis on studying the molecular events that underlie radiation-induced tumorigenesis, particularly in the context of brain and skin cancers. Her current research interests include exploring the non-cancerous effects induced by radiation exposure within the central nervous system and the lens. She is actively involved in the SEAWave project.

EMILIANO FRATINI was born in Rome, Italy, in 1982. He received the bachelor's degree (B.Sc.) and master's (M.Sc.) degrees in biology from the University of "Roma TRE," Rome, Italy, in 2005 and 2007, respectively, and the Ph.D. degree in molecular and cell biology from the University of "Roma TRE," Rome, Italy, in 2010. Recently, he has attained a post graduate course in bioinformatics from the University of Rome "Sapienza," Rome, Italy, in 2023. He is currently a Researcher in the field of radiation biology with a background in molecular and cell biology and cancer research. His Ph.D. thesis focused on the identification of molecular processes in the skin after in vivo irradiation with neutrons. He was a research Fellow with Enrico Fermi Study and Research Center during 2011–2014, as part of the unit of Health and Technology at Istituto Superiore di Sanità, he has carried out research to develop a combined description of molecular and cellular response to low doses of ionizing radiation in a multicellular contest, taking advantage of a good knowledge of specific techniques. At the same time, he focused on the cosmic silence project studying the effects of the reduction of natural environmental radiation, analyzing the molecular mechanisms involved in the biological response of living systems to natural environmental ionizing radiation. He had a military experience as Lieutenant junior grade (LTJG) in the Italian Military Navy/Coast Guard during 2014–2017. He is with the Health Protection Technologies Division, ENEA, Rome, Italy. He is actively involved in the SEAWave Project. Dr. Fratini is a member of the European Radiation Research Society (ERRS).

SIMONETTA PAZZAGLIA was born in Rome, Italy, in 1962. She received the graduation degree in biological sciences from the University "La Sapienza," Rome, in 1988. In 1991, she was a Postdoctoral Fellow with the Department of Human Oncology, University of Wisconsin, Hospital and Clinics, Madison, WI, USA. Between 1993 and 2003, she held the position of junior Scientist with ENEA, focusing on the design and execution of experimental projects in the field of radiation biology. Since 2004, she has held the position of senior Scientist and currently is the Head of the Biomedical Technologies Laboratory, ENEA, where she oversees and coordinates various research teams. She has actively engaged in numerous international collaborations, assuming significant roles in EU-funded collaborative projects spanning from FP3 to FP7, and in H2020 initiatives. She is actively involved in the SEAWave project. She has authored or coauthored extensively in the scientific literature, and she is reviewer for the major journals in her research area. She has authored or coauthored more than 90 scientific publications. Dr. Pazzaglia is member of the Italian Society for Radiation Research (SIRR) and of the Radiation Research Society (RRS), USA. Since 2014, she has been a key member of the expert group contributing to the Strategic Agenda of MELODI (Multidisciplinary European Low Dose Initiative), a European platform dedicated to research on the risks associated with low dose ionizing radiation.

MARIATERESA MANCUSO was born in Catanzaro, Italy, in 1965. She received the bachelor's degree (B.Sc.) in biological sciences from the University "La Sapienza," Rome, in 1990, discussing a thesis on the biological effects of gaseous pollutants administered by inhalation route. In the post-graduate years, she has gained experience in radiobiology, molecular carcinogenesis and toxicology as well as deep knowledge of experimental animal models for chemical- and radiation-induced tumourigenesis, together with a strong experience in histology, electron microscopy, pathology, molecular pathology and molecular biology. Since 2001, she has been a permanent staff with ENEA. From 2019 to 2023, she was the Head of the Biomedical Technologies Laboratory, ENEA, and she is currently the Head of the Division Health Protection Technologies at ENEA. Dr. Mancuso is honorary Professor of molecular biology and histology. She has authored or coauthored more than 100 peer reviewed articles and is reviewer for many journals in her research area. She has been a coordinator or team member in EU projects (FP6, FP7 and H2020) as well as in several national projects. In SEAWave, she is the Leader of the WP "Animal Study on Skin Carcinogenicity and Other Endpoints of FR2 Exposure". She is a member of the Radiation Research Society (RRS), USA.

THEODOROS SAMARAS (Member, IEEE) received the degree in physics from the Aristotle University of Thessaloniki, Thessaloniki, Greece, in 1990, the M.Sc. degree in medical physics (with distinction) from the University of Surrey, Surrey, U.K., in 1991, and the Ph.D. degree from the Aristotle University of Thessaloniki, in 1996. In 1998, he joined the Swiss Federal Institute of Technology (ETH) in Zurich, Zurich, Switzerland, where he was mainly involved in studying the effect of heat diffusion in electromagnetic dosimetry. He subsequently moved to the Hyperthermia Unit of the Erasmus Medical Center of Rotterdam, with a Marie-Curie postdoc fellowship from the European Commission. In 1999, he returned as a faculty member to the Aristotle University of Thessaloniki, where he is currently a Professor in applied electromagnetics and bioelectromagnetics. His research interests include biomedical applications and the safety of electromagnetic fields. Prof. Samaras is a member of the BioEM Society and the Editor-In-Chief of Wiley's *Bioelectromagnetics*. He is also a member of the European Commission's Scientific Committee on Health, Environmental and Emerging Risks (SCHEER).